1 # Contrasting impacts of humidity on the ozonolysis of
2 # monoterpenes: insights into the multi-generation
3 # chemical mechanism

4

5 Shan Zhang, Lin Du*, Zhaomin Yang, Narcisse Tsona Tchinda, Jianlong Li, Kun Li*

6 Environment Research Institute, Shandong University, Qingdao 266237, China.

7 *Correspondence to*: Lin Du (lindu@sdu.edu.cn) and Kun Li (kun.li@sdu.edu.cn)

8

9 **Abstract.** Secondary organic aerosol (SOA) formed from the ozonolysis of biogenic monoterpenes is a

10 major source of atmospheric organic aerosol. It has been previously found that relative humidity (RH)

11 can influence the SOA formation from some monoterpenes, yet most studies only observed the increase

12 or decrease in SOA yield without further explanations of molecular-level mechanisms. In this study, we

13 chose two structurally different monoterpenes (limonene with an endocyclic double bond and an

14 exocyclic double bond, Δ^3-carene with only an endocyclic double bond) to investigate the effect of RH

15 in a set of oxidation flow reactor experiments. We find contrasting impacts of RH on the SOA formation:

16 limonene SOA yield increases by ~100% as RH increases, while there is a slight decrease in Δ^3-carene

17 SOA yield. By analyzing SOA chemical composition and reaction mechanisms, the enhancement in

18 limonene SOA yield can be attributed to the water-influenced reactions after ozone attack on the

19 exocyclic double bond of limonene, which leads to the increment of lower volatile organic compounds

20 under high RH condition. However, as Δ^3-carene only has an endocyclic double bond, it cannot undergo

21 such reactions. This hypothesis is further proved by the SOA yield enhancement of β-caryophyllene, a

22 sesquiterpene that also has an exocyclic double bond. These results greatly improve our understanding

23 of how water vapor influences the ozonolysis of biogenic organic compounds and subsequent SOA

24 formation processes.

25 **1 Introduction**

26 　　Secondary organic aerosol (SOA), as an important type of ambient fine particulate matter (PM$_{2.5}$:

27 aerosols with aerodynamic diameter ≤ 2.5 μm) (Guo et al., 2014; Huang et al., 2014), has caused a series

28 of negative impacts on human health (Pye et al., 2021), air quality (Zhang et al., 2016) and global climate

29 (Levy et al., 2013). SOA produced from the oxidation of biogenic volatile organic compounds (BVOCs)

30 is a major component of SOA in heavy forest regions during summer (Sindelarova et al., 2014; Ahmadov

31   et al., 2012), and contributes by a large fraction (~40%-80%) to global OA budget (Cholakian et al.,

32   2019).

33   Monoterpenes, mostly emitted from coniferous trees, account for ~11% in total BVOCs

34   (Sindelarova et al., 2014; Kanakidou et al., 2005). Limonene is one of the most abundant monoterpenes,

35   with the annual emission budget of 11.4 Tg yr^{-1} (Guenther et al., 2012). Apart from the biogenic source,

36   limonene can also be released from the indoor emission, mainly from essential oils (Ravichandran et al.,

37   2018; De Matos et al., 2019; Mot et al., 2022). Limonene has an endocyclic double bond and an exocyclic

38   double bond, and is thus more reactive than other monoterpenes towards oxidants such as ozone (O_3),

39   hydroxyl radical (OH), and nitrate radical (NO_3) (Chen and Hopke, 2010; Atkinson and Arey, 2003). Δ^3-

40   carene is another kind of monoterpene that dominates the monoterpene emission from Scots pine (Bäck

41   et al., 2012). Different from limonene, Δ^3-carene contains only one endocyclic double bond, which is

42   similar to most other monoterpenes.

43   Ozonolysis is an important reaction pathway for limonene and Δ^3-carene. Although reactions with

44   OH and NO_3 are faster than that with O_3 for both two monoterpenes (Atkinson, 1991; Khamaganov and

45   Hites, 2001; Chen et al., 2015; Shaw et al., 2018), the atmospheric concentration of the latter

46   monoterpene is much higher than that of the former (Sbai and Farida, 2019). The contributions of O_3-

47   reactions with limonene and Δ^3-carene to tropospheric degradation are 47% and 24%, respectively, in

48   the daytime (Ziemann and Atkinson, 2012). In pristine areas where NO_3 concentration is very low,

49   ozonolysis is also the dominant fate for limonene and Δ^3-carene in the nighttime. In addition, it has been

50   previously found that the ozonolysis of monoterpenes can produce more extremely low volatility

51   products than OH-initiated oxidation, which contributes by a large fraction to the SOA production

52   (Jokinen et al., 2015). For either limonene or Δ^3-carene, the first step for ozonolysis is attacking on the

53   endocyclic double bond to form two types of stabilized Criegee intermediates (sCI) with low energy (Fig.

54   S1) (Drozd and Donahue, 2011; Chen et al., 2019). The sCI will then trigger a series of chemical reactions,

55   like isomerization, decomposition and addition reactions. Correspondingly, the major components in Δ^3-

56   carene SOA are caric acid, OH-caronic acid, and caronic acid (Ma et al., 2009; Thomsen et al., 2021),

57   while the major components from limonene SOA are limonaldehyde, keto-limonon aldehyde, limononic

58   acid and keto-limononic acid (Pathak et al., 2012; Wang and Wang, 2021).

59   Water is ubiquitous in the atmosphere and can affect the formation mechanism of SOA and its

60   relevant physical and chemical properties (Sun et al., 2013). A number of field measurements have shown

61   that the average molecular weight of the water/organic phase and activity coefficient of condensed

62   organics would be changed due to the change of relative humidity (RH) (Seinfeld et al., 2001; Li et al.,

63   2020). In addition, several laboratory studies have demonstrated that RH can influence the ozonolysis of

64   monoterpenes in different ways. Most of those studies have reported either an inhibitory effect or a

65   negligible effect of high RH on the particle formation (Bonn and Moortgat, 2002; Fick et al., 2002; Zhao

66   et al., 2021; Ye et al., 2018). Nevertheless, few other studies found that high RH can promote SOA

67   formation from the ozonolysis of limonene (Yu et al., 2011; Gong et al., 2018; Xu et al., 2021), but the

68   reason of this promotion effect remains unclear.

69   To fully examine the effects of water on SOA formation from the ozonolysis of monoterpenes,

70   especially the related chemical processes, we used an oxidation flow reactor (OFR) to investigate the

71   ozonolysis of limonene and Δ^3-carene under different RH conditions in this study. An ultra-high

72   performance liquid chromatography with a quadrupole time-of-flight mass spectrometer (UPLC-Q-TOF-

73   MS) was deployed to analyze the molecular chemical composition of the SOA, which provided insights

74   into the physical and chemical processes influenced by the water content. With these state-of-the-art

75   techniques, we proposed mechanisms that may explain the inhibitory or enhancing RH effects on SOA

76   formation for different monoterpenes.

77   **2 Experimental methods**

78   **2.1 Oxidation flow reactor experiments**

79   A series of dark ozonolysis experiments of limonene and Δ^3-carene were conducted in a custom-

80   made oxidation flow reactor (OFR). The OFR is a 602 cm long stainless cylinder with a volume of 2.5 L

81   (Fig. S2). A zero-air generator (XHZ2000B, Xianhe, China) was used to generate dry clean air as the

82   carrier gas for the OFR. As shown in Fig. S2, there are four gas paths upstream of the OFR: the first path

83   is the precursor gas channel through which monoterpenes are injected via a syringe pump (ISPLab 01,

84   Shenchen, China); the second path is for the flow of 300 sccm dry zero air passing through a mercury

85   lamp ($\lambda = 185$ nm) to generate O_3; the third path is connected to a water bubbler to generate wet air; the

86   fourth path is the extra dry zero air entering the OFR. The RH in the OFR was controlled by adjusting

87   the ratio of the wet and dry zero air flows. A water recycle system was equipped to keep the temperature

88 (T) around at 298 K. The total flow was 0.9 L min^{-1}, resulting in an average residence time of 167 s. The

89 RH and T in the OFR were monitored by a T/RH Sensor (HM40, VAISALA, Finland). The concentration

90 of ozone and the consumption of the precursor gas were measured with an ozone monitor (Model 106L,

91 2B Technologies, USA) and a gas chromatography with flame ionization detector (GC-FID 7890B,

92 Agilent Technologies, USA), respectively. The GC was equipped with a DB-624 column (30 m × 0.32

93 mm, 1.8 µm film thickness) whose temperature was set to ramp from 100 ℃ to 180 ℃ at a rate of 20 ℃

94 min^{-1}, and then held at 180 ℃ for 2 min. Before each experiment, O_3 was introduced into the OFR to

95 clean it until the background aerosol mass concentration reached < 1 µg m^{-3}.

96   The experimental conditions are shown in Table 1. In these OFR experiments, the precursor

97 (limonene or Δ^3-carene) concentration was set to ~320-340 ppb. A high O_3 concentration of ~6 ppm was

98 used to realize an equivalent aging time of 0.41 day in the real atmosphere, assuming an average ambient

99 O_3 concentration of 28 ppb (Sbai and Farida, 2019) (see section S1 for the calculation). Under such

100 conditions, most of the precursors were consumed, since the residence time was almost five and three

101 times of the half-life for limonene and Δ^3-carene, respectively. A series of RH conditions ranging from

102 dry (1-2%) to 60% with a step of ~10% were used to investigate the effects of water content on SOA

103 production and composition (see Table 1). All materials used in this experiment have been described in

104 S2.

105 **Table 1.** Experimental conditions and results.

Exp.	[Precursor] (ppb)	[O]$_3$ (ppm)	T (K)	RH (%)	N$_{(13.8\text{-}723.4\ nm)}$[a] (cm^{-3})	M$_{(13.8\text{-}723.4\ nm)}$[b] (µg m^{-3})	D$_{(mean)}$[c] (nm)	SOA yield (%)
				limonene				
1	321±39	5.7	298	1–2	6.9×10^5	980.9	138.2	62.9
2	321±39	6.0	298	10±2	1.3×10^6	1377.5	126.8	88.4
3	321±39	5.9	298	20±2	9.0×10^5	1573.3	150.9	90.2
4	321±39	5.9	298	30±2	1.4×10^6	1573.3	128.9	100.9
5	321±39	6.0	298	40±2	1.7×10^6	2051.4	130. 7	131.6
6	321±39	5.5	298	50±2	1.5×10^6	1962.7	137.8	125.9
7	321±39	5.5	298	60±2	1.5×10^6	2211.1	139.0	141.8

				Δ^3-carene				
8	341±28	6.1	298	1–2	9.5×10^4	346.0	195.8	19.4
9	341±28	6.4	298	10±2	1.4×10^5	300.3	163.4	16.8
10	341±28	6.4	298	20±2	9.4×10^4	244.9	176.9	13.7
11	341±28	6.0	298	30±2	5.9×10^4	241.2	205.1	13.5
12	341±28	6.3	298	40±2	4.6×10^4	205.8	203.2	11.5
13	341±28	6.3	298	50±2	6.8×10^4	196.7	180.7	11.0
14	341±28	6.3	298	60±2	5.6×10^4	198.5	190.2	11.1

[a] $N_{(14.1\text{-}735\ nm)}$ means the total particle number concentration from size 13.8 nm to 723.4 nm. [b] $M_{(13.8\text{-}723.4\ nm)}$ means the total particle mass concentration from size13.8 nm to 723.4 nm. [c] $D_{(mean)}$ means the particle mean diameter.

2.2 SOA particle analysis

2.2.1 SOA yield

The SOA particle size distribution was measured with a scanning mobility particle sizer (SMPS), which consists of a differential mobility analyzer (DMA) (model 3082, TSI Inc., USA) and a condensation particle counter (CPC) (model 3776, TSI Inc., USA). The samples were measured by SMPS every 5 minutes with a sampling flow and a sheath flow of 0.3 L min^{-1} and 3 L min^{-1}, respectively. The SOA mass concentration was calculated from the volume concentration measured with SMPS and the aerosol density, which was estimated to be 1.25 cm^{-3} for limonene- and 1.09 g cm^{-3} for Δ^3-carene-SOA (Thomsen et al., 2021; Watne et al., 2017).

The SOA yield (Y) for individual organic gas can be calculated as:

$$Y=\frac{\Delta M}{\Delta HC}$$

Where ΔM is the total mass concentration of SOA, ΔHC is the mass concentration of reacted precursor (Ng et al., 2007; Odum et al., 1996).

2.2.2 Ultra-high performance liquid chromatography quadrupole time-of-flight mass spectrometry analysis

An ultra-high performance liquid chromatography (UPLC, UltiMate 3000, Thermo Scientific) coupled with a quadrupole time-of-flight mass spectrometry (Q-TOFMS, Bruker Impact HD) was used to analyze the molecular-level chemical composition of SOA. First, the SOA particles were collected on

5

127   the PTFE filters (47 mm diameter, 0.22 µm pore size, Jinteng, China). Next, these filters were dissolved

128   and extracted by 5 mL methanol for two times. Extracts were then filtered through PTFE syringe filters

129   (0.22 µm pore size), and were concentrated to near dryness by nitrogen-blowing. At last, the samples

130   were redissolved in a 200 µL solution with 0.1% (v/v) formic acid in 50:50 methanol/ultrapure water

131   mixture.

132   The parameters of LC-MS were set as follows: capillary voltage 4000 V, nebulizer pressure 0.4 bar,

133   dry heater temperature 200℃, end plate voltage −500 V, and flow of dry gas 4 L min^{-1}. A C$_{18}$ column

134   (100 Å, 3 mm particle size, 2.1 mm×50 mm, Waters, USA) was used with a column temperature of 35℃.

135   The mobile phase was 0.1 % formic acid in methanol (A) and 0.1 % formic acid in ultra-high purity

136   water (B) with a flow of 200 µL min^{-1}. The injection volume was 5 µL. The MS was operated in negative

137   ion mode, and the detection molecular weight range was from m/z 50 to 1500.

3 Results and discussion

3.1 SOA production under different RH conditions

140   SOA formation of a representative experiment is shown in Fig. S3. It is found that the formed SOA

141   are mainly in the size range of 60-200 nm, and the number concentration and mass concentration are

142   relatively stable during the course of the OFR experiment. SOA formation from limonene and Δ^3-carene

143   in terms of particle number concentration, particle mass concentration, and SOA yield as a function of

144   RH are illustrated in Fig. 1a-c. We find that all the above-mentioned 3 parameters of limonene-SOA

145   increase with the increasing RH. The increment of particle mass concentration and SOA yield from the

146   ozonolysis of limonene is ~100% higher at wet (60% RH) than at dry conditions. In contrast, SOA

147   formation from Δ^3-carene is suppressed by ~40% under high RH. The distinct effects of RH on SOA

148   formation from the ozonolysis of limonene and Δ^3-carene found in this study agree with most previous

149   studies (Yu et al., 2011; Jonsson et al., 2006b; Bonn et al., 2002; Gong and Chen, 2021; Li et al., 2019b).

150   As shown in Table 2, Yu et al. (2011) reported a positive correlation between SOA production and RH

151   for the ozonolysis of limonene in the chamber experiments without OH scavenger. Their experimental

152   condition is similar to that in our study regarding the absence of OH scavenger and, thus, similar results

153   were observed. However, in the presence of OH scavenger, results are quite different. Jonsson et al. (2006)

154   observed a similar enhancement effect of high RH on SOA production with 2-butanol as the OH

155   scavenger, while Bonn et al. (2002) found a negligible or suppressive effect with cyclohexane as the OH

156   scavenger. It should be noted that the OH scavenger not only has the ability to scavenge OH but also

157   produces additional products which may influence the reactions of target precursors. According to

158   previous studies, the influence of different OH scavengers can vary (Jonsson et al., 2008). This may

159   explain the different findings with and without OH scavenger for limonene-SOA. With regard to Δ^3-

160   carene, similar results are found in the absence of OH scavenger, namely, high RH has negligible or

161   slightly suppressive effect on SOA production (Bonn et al., 2002; Fick et al., 2002). Same as limonene,

162   the presence of OH scavenger and its different chemical nature can explain the different results found

163   previously (Jonsson et al., 2006a; Bonn et al., 2002).

164   The enhancement in limonene-SOA production under high RH can be due to several reasons from

165   either physical or chemical processes. First, the hygroscopic growth of the particles (i.e., absorption of

166   water content) can lead to higher mass concentration under higher RH, but the enhancement should be

167   at most ~30% as the growth factor (GF, the ratio of wet and dry diameter: $D_{wet/Ddry}$) of limonene-SOA is

168   ≤1.1 (Varutbangkul et al., 2006). However, we do not observe an obvious change in the mean diameter

169   when comparing dry and wet conditions (Fig. 1d). In addition, hygroscopic growth should also occur for

170   Δ^3-carene SOA, but no obvious enhancement in particle mass is observed (Fig. 1a). Therefore, it is

171   suggested that physical processes regarding hygroscopic growth play a minor role in the enhancement in

172   limonene-SOA under high RH. As a consequence, we believe that chemical processes are likely the

173   reason of the enhancement in limonene-SOA under high RH. Water can influence chemical processes in

174   the gas phase or in the particle phase. Particle-phase reactions can promote the growth of small particles

175   and, thus, mainly lead to larger particle sizes. As the observed SOA enhancement is mainly from high

176   number concentration particles rather than the large size particles (Fig. 1b and 1d), it is likely that the

177   water-participated gas-phase reactions are the most possible reasons for the limonene-SOA enhancement.

178   The reaction mechanism is analyzed below based on the mass spectra information on the SOA.
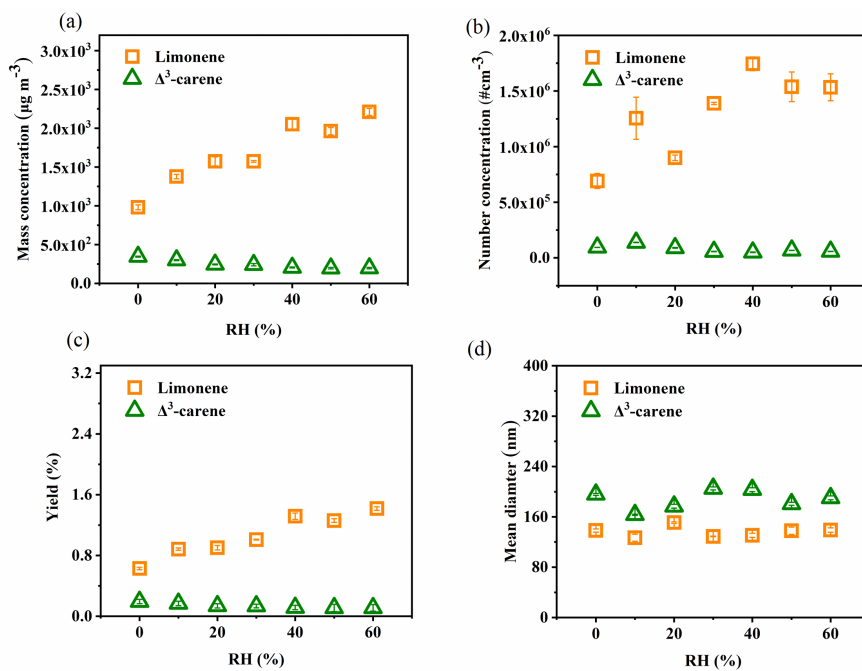
Figure 1. The effect of RH on the SOA formation: (a) number concentration, (b) mass concentration, (c) SOA yield, (d) mean diameter.

183

Table 2. Comparison with previous studies on the effect of RH.

| Precursor	Concentration (ppb)	Reactor	OH scavenger	T (K)	RH (%)	M[a]	N[b]	Reference
limonene	1000	flow reactor	cyclohexane	295±2	0.02 and 32.5	no effect	–[e]	Bonn et al. (2002)
	320	chamber	N.M.[c]	296±2	18±2, 50±3 and 82±2	+[d] (7 times)	+[d] (8 times)	Yu et al. (2011)
	15 and 30	flow reactor	2-butanol	298±0.4	< 2-85	+[d]	+[d]	Jonsson et al. (2006)
	exocyclic (15.2) and endocyclic (24.6)	flow reactor	2-butanol	298	10-50	exocyclic (+[d]) and endocyclic (–[e])	N.M[c]	Gong and Chen (2021)
	1085	flow reactor	none	298	3-62	+[d]	–[e]	Li et al. (2019)
	321±39	flow reactor	none	298	0-60	+[d] (2 times)	+[d] (3 times)	this study
Δ^3-carene	1000	flow reactor	cyclohexane	295±2	0.02 and 32.5	no effect	–[e]	Bonn et al. (2002)
	14.2 and 29.4	flow reactor	2-butanol	298±0.4	< 2-85	+[d]	+[d]	Jonsson et al (2006)
	1111	flow reactor	none	298	3-62	–[e]	–[e]	Li et al. (2019)
	341±28	flow reactor	none	298	0-60	–[e]	no effect	this study

184

185

[a] M means total particle mass concentration. [b] N means total particle number concentration. [c] N.M. means not mentioned. [d] Positive sign (+) means the mass or number concentration increases with RH. [e] Negative sign (–) means the mass or number concentration decreases with RH.

3.2 Molecular analysis of SOA particles

186

187   The UPLC/ESI-Q-TOF-MS was used to examine the SOA molecular composition under high and

188   low RH conditions. As shown in Fig. 2a, the mass spectra of limonene-SOA are divided into four groups:

189   monomeric group (<m/z 300), dimeric group (m/z 300-500), trimeric group (m/z 500-700), and

190   tetrameric group (m/z 700-1000), corresponding to products containing one, two, three, and four

191   oxygenated limonene units, respectively (Bateman et al., 2009). Most of the SOA molecules are

192   monomers (>60%) (Fig. 2b) and dimers (~25%), while trimers and tetramers contribute to very small

193   fractions (<10% and ~3%) (Table S1). Although the SOA mass concentration increases by ~100% under

194   high RH condition, the relative intensities of MS peaks do not significantly change with varying RH

195   conditions. In other words, we did not observe an obvious change in the overall MS patterns, and the

196   fractions of the four groups only slightly differed under different RH conditions, e.g., the fraction of

197   monomers was 62% under dry condition and 66% under wet conditions. However, if we take a closer

198   look, the intensities and contributions of specific peaks are quite different with varying RH. For example,

199   the relative intensity of $C_{10}H_{16}O_2$, a possible first-generation product (Gong et al., 2018), decreases by

200   ~20% with increasing RH from dry to 60% (Table S2). This is likely due to the multi-generation reactions

201   influenced by water vapor concentration, as discussed below with the proposed reaction mechanism of

202   limonene ozonolysis.

203
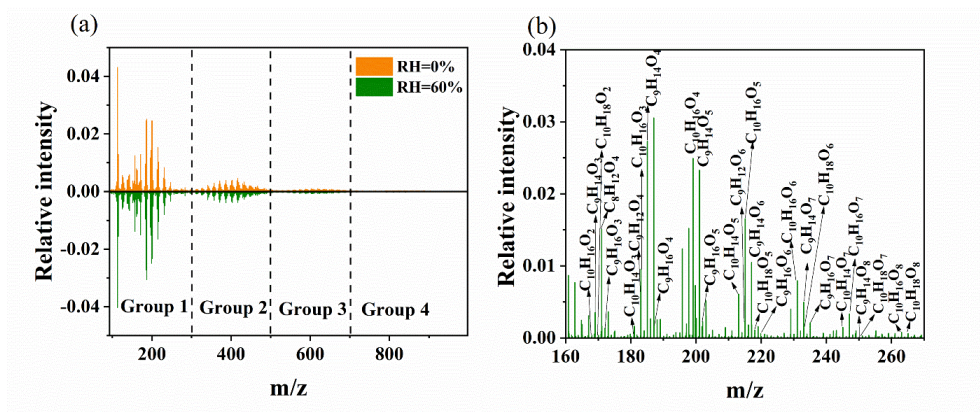
Figure 2. UPLC/ (−) ESI-Q-TOF-MS mass spectra of SOA from limonene ozonolysis. (a) MS under

204

high and low RH conditions; (b) the identification of monomers under high RH condition.

205

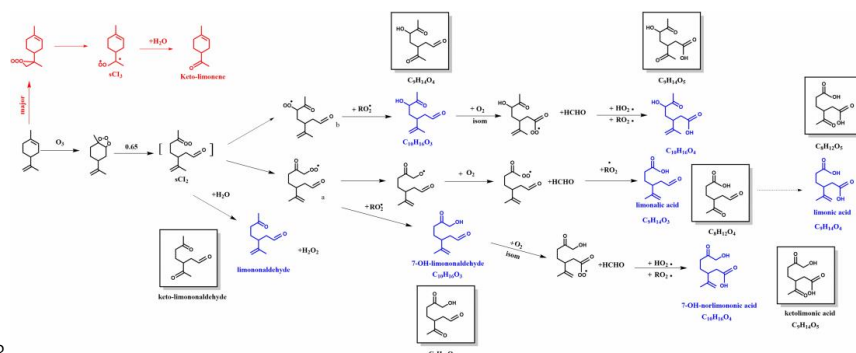206   The proposed reaction mechanism of limonene ozonolysis is shown in Fig. 3 and Fig. 4. The initial

207   step in the reaction of O_3 with limonene is the attack of the endocyclic double bond to form sCI_1 and sCI_2

208   (with branching ratios of 0.35 and 0.65, respectively). There are four reaction pathways for sCI_1 in the

209   next steps (Fig. 3). The first pathway is the reaction with H_2O, alcohol or carboxylic acid to form a

210   carboxylic acid species with hydroxyl, which would subsequently lose a molecule of water to form

211   limononaldehyde or lose a molecule of hydrogen peroxide to form limononic acid (Grosjean et al., 1992;

212   Li et al., 2019b). The second and third pathways are reactions with carboxylic acids and carbonyls,

213   respectively, generating anhydrides and secondary ozonides. The fourth way is the loss of a hydroxyl

214   radical (·OH) to generate an alkyl radical (R·), $C_{10}H_{15}O_2$·. Meanwhile, the produced ·OH can attack

215   limonene to form another alkyl radical $C_{10}H_{17}O$·. These alkyl radicals react with O_2 and form peroxy

216   radicals (RO_2·). The atmospheric fate of produced RO_2· in the absence of NO_x includes the reaction with

217   RO_2· or HO_2· (Atkinson and Arey, 2003) and the unimolecular H shift. The RO_2·+ HO_2· route mainly

218   form hydroperoxide (ROOH), and the minor fraction is to form alcohols and carbonyls (Atkinson and

219   Arey, 2003). The products of bimolecular reactions between RO_2· and RO_2· are alcohols, carbonyls,

220   alkoxy radicals, peroxides and ROOR dimers (Hammes et al., 2019; Peng et al., 2019). The H shift of

221   RO_2· can form second-generation R· and trigger a main generation channel of highly oxidized molecules

222   (HOMs), i.e., R· would go through a process of repeated oxygen addition and hydrogen-atom shift to

223   form HOMs with high O/C ratios of > 0.7–0.8 (Molteni et al., 2018; Bianchi et al., 2019).

224   In addition to the sCI_1 route, many products can be formed from the sCI_2 route (Fig. 4). First, sCI_2

225   reacts with H_2O and decomposes to limononaldehyde and H_2O_2. Additionally, sCI_2 could experience an

226   O_2 addition, ·OH loss and isomerization to produce two types of RO_2·, which can undergo the similar

227   reactions as the RO_2· formed from the sCI_1 route, and the major products are also shown in Fig. 4.

228   Since limonene and Δ^3-carene both have an endocyclic double bond, the similar reactions as

229   mentioned above can occur for the ozonolysis of Δ^3-carene (Fig. S4), and most corresponding formula

230   in Fig. S4 could be identified in Table S3. However, the reactivity of limonene towards O_3 is expected to

231   be higher owing to its exocyclic double bond. As shown in Fig. 4, the attack of O_3 to the exocyclic double

232   bond mainly leads to sCI_3 (highlighted in red) with the unpaired electrons outside the ring (Leungsakul

233   et al., 2005). sCI_3 can react with H_2O to form a carbonyl called keto-limonene. It should be noted that

234   this reaction can occur not only for limonene, but also for all the products that retain the exocyclic double

235   bond. As a result, the compounds that are colored in blue in Fig. 3 and Fig. 4 can undergo further reactions

236   to generate products with an additional carbonyl (see the boxes in Fig. 3 and Fig. 4). Furthermore, their

237   molecular formula shown in Table S4 have been identified using the Q-TOF-MS. This mechanism can

238   well explain the decrease in the relative intensity of $C_{10}H_{16}O_2$ and the increase in the relative intensity of

239    $C_9H_{14}O_3$ (Table S2)

Figure 3. Proposed formation mechanism for SOA formation from sCI oxidation under high RH. The compounds in blue and in boxes are identified using UPLC/ (−) ESI-Q-TOF-MS.

Figure 4. Proposed formation mechanisms for SOA formation from sCI_2 and sCI_3 oxidation under high RH. The compounds in blue and in boxes are identified using UPLC/ (−) ESI-Q-TOF-MS.

3.3 Processes leading to the increase or decrease in SOA formation

Based on the results and mechanisms shown above, we present evidence that high humidity enhances limonene-SOA formation. First, the presence of water vapor enhances the formation of carbonyls from the reaction of exocyclic double bond. The oligomerization of these carbonyls generates more dimers. As shown in Table S1, 25 more dimers (187 dimers vs 162 dimers) were found under high RH condition compared to those under low RH condition. These dimers can be classified as low-volatile organic compounds (LVOC; $3 \times 10^{-4} < C_0 < 0.3$ µg m^{-3}) and extremely low-volatile organic compounds (ELVOCs; $C_0 < 3 \times 10^{-4}$ µg m^{-3}) (Fig. 5a), and thus promote the nucleation and new particle formation in different ways. This finding is similar to that from a previous study showing that high RH can promote dimer formation from the ozonolysis of α-pinene (Kristensen et al., 2014). Second, we find that high RH can also promote the formation of HOMs, although the mechanism remains unclear. As shown in Table S2, many HOMs are detected under high RH condition but not detected under low RH condition, including both monomers and dimers. HOMs have low volatilities and, thus, can also promote new particle formation. Overall, the promoted dimer and HOM formation greatly enhance the new particle number concentration under high RH condition (Fig. 6).
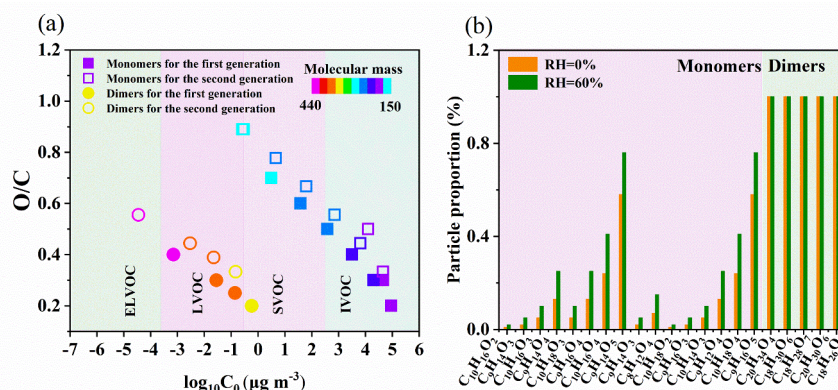
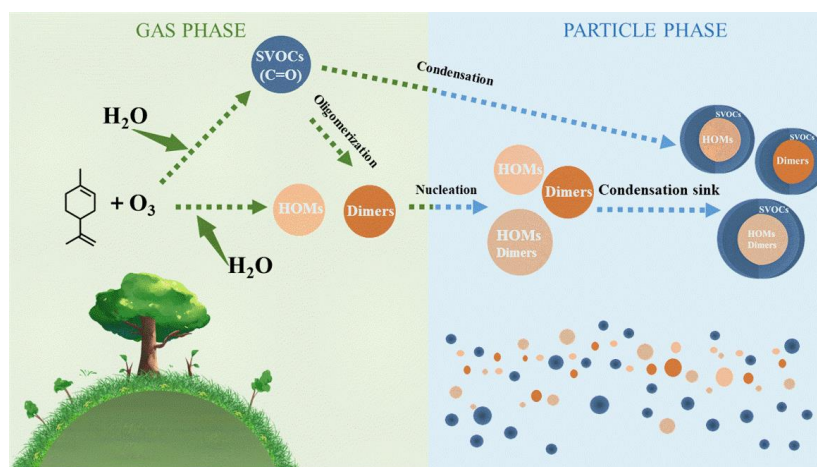**Figure 5.** (a) Distribution of the limonene-SOA in the two-dimensional volatility basis set (2D-VBS)
space. (b) Partitioning coefficients of limonene monomers and dimers under low and high RH conditions.

Figure 6. Schematic diagram of the possible mechanisms for the enhancement of limonene-SOA.

High particle number concentration generally provides more surface areas for semi-volatile organic
compounds (SVOCs; $0.3 < C_0 < 300$ μg m^{-3}) to condense on, which results in higher condensation sink
(CS). In the OFR, the fates of SVOCs include condensing on aerosol, getting lost on the wall, and reacting
with OH radicals to form functionalization and/or fragmentation products (Palm et al., 2016; Li et al.,
2019a). The promoted condensation by higher CS leads to a higher fraction of SVOCs getting into the
particle phase rather than getting lost on the wall or becoming smaller fragments staying in the gas phase,

276 and thus promoting SOA formation (Li et al., 2019a). Furthermore, the transformation from C-C double

277 bond to carbonyl shown in Fig. 3 and Fig. 4 decreases the volatility of molecules, which can largely

278 influence the gas-particle partitioning of the monomeric compounds (Fig. 5b). For example, the C_0 values

279 of $C_{10}H_{16}O_2$ and $C_{10}H_{16}O_3$ are 90701 and 19968 µg m^{-3}, corresponding to partitioning coefficients of

280 0.01 and 0.05, respectively (Fig. 5b and Table S2), with an SOA mass concentration of ~1000 µg m^{-3}

281 under dry condition. When they are converted to carbonyls $C_9H_{14}O_3$ and $C_9H_{14}O_4$, the values of C_0

282 become 45556 and 6479 µg m^{-3}, corresponding to partitioning coefficients of 0.02 and 0.13, respectively

283 (Fig. 5b and Table S2), with the same SOA loading. This enhancement in partitioning coefficient can

284 largely promote the condensation of SVOCs and, thus, enhance the SOA mass concentration. In addition,

285 the enhanced SOA formation can further influence the equilibrium, e.g., the partitioning coefficient of

286 $C_{10}H_{16}O_3$ increases from 0.05 to 0.10 when SOA mass concentration increases from ~1000 µg m^{-3} under

287 dry condition to ~2000 µg m^{-3} under wet condition (Fig. 5b and Table S2). The distribution of saturation

288 vapor pressure for monomers and dimers identified by MS has also been shown in Fig. 5a. As can be

289 seen from this figure, around 50% monomers are categorized as SVOCs, thus having the large fraction

290 in the particle phase when converting from dry to wet conditions. Overall, the different fate and

291 partitioning of SVOCs largely enhance the amount of SVOCs in the particle phase (Fig. 6).

292 Concluding the analysis above, high humidity promotes the SOA formation from the ozonolysis of

293 limonene in two steps: nucleation of new particles and condensation of SVOCs on them (Fig. 6). These

294 two steps are closely related to the multi-generation reactions of the exocyclic C=C bond, which are

295 unlikely to happen for the ozonolysis of Δ^3-carene. In a recent study by Gong and Chen (Gong and Chen,

296 2021), it was found that high RH can inhibit the SOA formation from the first-generation oxidation of

297 limonene ozonolysis, but enhance the SOA formation from the second-generation oxidation. Their results

298 agree well with the results and analysis shown here.

299 Regarding Δ^3-carene, the mechanisms and processes are almost opposite to those of limonene. First,

300 water vapor reacts with sCI_1 or sCI_2 to promote the formation of α-hydroxyalkyl-hydroperoxides (Fig.

301 S4). Their subsequent products without second ozonolysis of exocyclic double bond have higher

302 volatility, and may most likely prevail in the gas phase. In addition, it has been found that α-hydroxyalkyl

303 hydroperoxides preferentially decompose into aldehydes and H_2O_2 (Kumar et al., 2014; Chen et al., 2016),

304 i.e., 3-caronaldehyde for Δ^3-carene, which has higher volatility than the products from other reaction

305   pathways. Correspondingly, the number and relative intensity of HOMs and dimers detected under high

306   RH conditions are both lower than those under low RH conditions (Table S5). As a result, high RH shows

307   an inhibitory effect on the SOA formation from Δ^3-carene ozonolysis.

308   To further confirm the assumption that water-influenced multi-generation reactions of the exocyclic

309   double bond enhance the SOA formation, we also conducted the β-caryophyllene ozonolysis experiments

310   under similar experimental conditions as limonene and Δ^3-carene (Table S6). Similar to limonene, β-

311   caryophyllene has an exocyclic C-C double bond that can undergo further reactions (Fig. S5). As

312   expected, we observe a large enhancement in SOA formation under high RH condition (Table S6 and

313   Fig. S6). This implies that monoterpenes, sesquiterpenes, and other BVOCs with two unsaturation double

314   bonds may follow similar reaction mechanisms during ozonolysis, and thus have a RH dependency in

315   SOA production.

4 Conclusions

In this study, the effect of humidity on SOA production from the ozonolysis of two monoterpenes (limonene and Δ^3-carene) was investigated with an OFR. Contrasting impacts of RH on the SOA formation were observed: limonene-SOA yield increases by ~100% when RH changes from ~1% to ~60%, while Δ^3-carene-SOA yield slightly decreases. By analyzing the chemical composition of SOA with ESI-Q-TOF-MS, we find that the multi-generation reactions of the exocyclic C-C double bond are likely the driving force of the enhancement in limonene-SOA. The presence of water promotes the formation of carbonyls from the reaction of exocyclic double bond, and further favors the formation of dimers and HOMs. This leads to promoted new particle formation and subsequent condensation of SVOCs. These reactions also lower the volatilities of the SVOCs, and further promote the gas-particle partitioning. Moreover, this hypothesis is proved by a similar behavior of the ozonolysis of β-caryophyllene (sesquiterpene with an exocyclic double bond) in SOA enhancement under high RH condition. The results in this study suggest that multi-generation reactions play an important role in SOA formation from the ozonolysis of BVOCs, which are significantly influenced by humidity. This impact is largely dependent on the molecular structure of the SOA precursors (e.g., with or without the exocyclic double bond), thus highlighting the importance to consider the molecular structure of monoterpenes in modeling and field studies of biogenic SOA.

18

344   2020QNQT012).

345   **Reference**

346   Ahmadov, R., McKeen, S. A., Robinson, A. L., Bahreini, R., Middlebrook, A. M., de Gouw, J. A.,

347   Meagher, J., Hsie, E. Y., Edgerton, E., Shaw, S., and Trainer, M.: A volatility basis set model for

348   summertime secondary organic aerosols over the eastern United States in 2006, J. Geophys. Res.-Atmos.,

349   117, D6301, https://doi.org/10.1029/2011JD016831, 2012.

350   Atkinson, R.: Kinetics and mechanisms of the gas-phase reactions of the NO_3 radical with organic

351   compounds, J. Phys. Chem. Ref. Data, 20, 459-507, https://doi.org/10.1063/1.555887, 1991.

352   Atkinson, R. and Arey, J.: Gas-phase tropospheric chemistry of biogenic volatile organic compounds: a

353   review, Atmos. Environ., 37, 197-219, https://doi.org/10.1016/S1352-2310(03)00391-1, 2003.

354   Bäck, J., Aalto, J., Henriksson, M., Hakola, H., He, Q., and Boy, M.: Chemodiversity of a Scots pine

355   stand and implications for terpene air concentrations, Biogeosciences, 9, 689-702,

356   https://doi.org/10.5194/bg-9-689-2012, 2012.

357   Bateman, A. P., Nizkorodov, S. A., Laskin, J., and Laskin, A.: Time-resolved molecular characterization

358   of limonene/ozone aerosol using high-resolution electrospray ionization mass spectrometry, Phys. Chem.

359   Chem. Phys., 11, 7931-7942, https://doi.org/10.1039/b905288g, 2009.

360   Bianchi, F., Kurtén, T., Riva, M., Mohr, C., Rissanen, M. P., Roldin, P., Berndt, T., Crounse, J. D.,

361   Wennberg, P. O., Mentel, T. F., Wildt, J., Junninen, H., Jokinen, T., Kulmala, M., Worsnop, D. R.,

362   Thornton, J. A., Donahue, N., Kjaergaard, H. G., and Ehn, M.: Highly oxygenated organic molecules

363   (HOM) from gas-phase autoxidation involving peroxy radicals: a key contributor to atmospheric aerosol,

364   Chem. Rev., 119, 3472-3509, https://doi.org/10.1021/acs.chemrev.8b00395, 2019.

365   Bonn, B. and Moortgat, G. K.: New particle formation during α- and β-pinene oxidation by O_3, OH and

366   NO_3, and the influence of water vapour: particle size distribution studies, Atmos. Chem. Phys., 2, 183-

367   196, https://doi.org/10.5194/acp-2-183-2002, 2002.

368   Bonn, B., Schuster, G., and Moortgat, G. K.: Influence of water vapor on the process of new particle

369   formation during monoterpene ozonolysis, J. Phys. Chem. A, 106, 2869-2881,

370   https://doi.org/10.1021/jp012713p, 2002.

371   Chen, H., Ren, Y., Cazaunau, M., Dalele, V., Hu, Y., Chen, J., and Mellouki, A.: Rate coefficients for the

372   reaction   of   ozone   with   2-and   3-carene,   Chem.   Phys.   Lett.,   621,   71-77,

373   https://doi.org/10.1016/j.cplett.2014.12.056, 2015.

374   Chen, L., Huang, Y., Xue, Y., Shen, Z., Cao, J., and Wang, W.: Mechanistic and kinetics investigations

375   of oligomer formation from Criegee intermediate reactions with hydroxyalkyl hydroperoxides, Atmos.

376   Chem. Phys., 19, 4075-4091, https://doi.org/10.5194/acp-19-4075-2019, 2019.

377   Chen, L., Wang, W., Wang, W., Liu, Y., Liu, F., Liu, N., and Wang, B.: Water-catalyzed decomposition

378   of   the   simplest   Criegee   intermediate CH_2OO,   Theor.   Chem.   Acc.,   135,   131,

379   https://doi.org/10.1007/s00214-016-1894-9, 2016.

380   Chen, X. and Hopke, P. K.: A chamber study of secondary organic aerosol formation by limonene

381   ozonolysis, Indoor Air, 20, 320-328, https://doi.org/10.1111/j.1600-0668.2010.00656.x, 2010.

382   Cholakian, A., Beekmann, M., Coll, I., Ciarelli, G., and Colette, A.: Biogenic secondary organic aerosol

383   sensitivity to organic aerosol simulation schemes in climate projections, Atmos. Chem. Phys., 19, 13209-

384   13226, https://doi.org/10.5194/acp-19-13209-2019, 2019.

385   de Matos, S. P., Teixeira, H. F., de Lima, Á. A. N., Veiga-Junior, V. F., and Koester, L. S.: Essential oils

386   and isolated terpenes in nanosystems designed for topical administration: a review, Biomolecules, 9, 138,

387   https://doi.org/doi:10.3390/biom9040138, 2019.

388   Drozd, G. T. and Donahue, N. M.: Pressure dependence of stabilized Criegee intermediate formation

389   from a sequence of alkenes, J. Phys. Chem. A, 115, 4381-4387, https://doi.org/10.1021/jp2001089, 2011.

390   Fick, J., Pommer, L., Andersson, B., and Nilsson, C.: A study of the gas-phase ozonolysis of terpenes:

391   the   impact   of   radicals   formed   during   the   reaction,   Atmos.   Environ.,   36,   3299-3308,

392   https://doi.org/10.1016/s1352-2310(02)00291-1, 2002.

393   Gong, Y. and Chen, Z.: Quantification of the role of stabilized Criegee intermediates in the formation of

394   aerosols in limonene ozonolysis, Atmos. Chem. Phys., 21, 813-829, https://doi.org/10.5194/acp-21-813-

395   2021, 2021.

396   Gong, Y., Chen, Z., and Li, H.: The oxidation regime and SOA composition in limonene ozonolysis: roles

397   of   different   double   bonds,   radicals,   and   water,   Atmos.   Chem.   Phys.,   18,   15105-15123,

398   https://doi.org/10.5194/acp-18-15105-2018, 2018.

399   Grosjean, D., Williams, E. L., and Seinfeld, J. H.: Atmospheric oxidation of selected terpenes and related

400   carbonyls: gas-phase   carbonyl   products,   Environ.   Sci.   Technol.,   26,   1526-1533,

401   https://doi.org/10.1021/es00032a005, 1992.

402   Guenther, A. B., Jiang, X., Heald, C. L., Sakulyanontvittaya, T., Duhl, T., Emmons, L. K., and Wang, X.:

403   The model of emissions of gases and aerosols from nature version 2.1 (MEGAN2.1): an extended and

404   updated framework for modeling biogenic emissions, Geosci. Model Dev., 5, 1471-1492,

405   https://doi.org/10.5194/gmd-5-1471-2012, 2012.

406   Guo, S., Hu, M., Zamora, M. L., Peng, J., Shang, D., Zheng, J., Du, Z., Wu, Z., Shao, M., Zeng, L.,

407   Molina, M. J., and Zhang, R.: Elucidating severe urban haze formation in China, Proc. Natl. Acad. Sci.

408   U. S. A., 111, 17373-17378, https://doi.org/10.1073/pnas.1419604111, 2014.

409   Hammes, J., Lutz, A., Mentel, T., Faxon, C., and Hallquist, M.: Carboxylic acids from limonene oxidation

410   by ozone and hydroxyl radicals: insights into mechanisms derived using a FIGAERO-CIMS, Atmos.

411   Chem. Phys., 19, 13037-13052, https://doi.org/10.5194/acp-19-13037-2019, 2019.

412   Huang, X., Yun, H., Gong, Z., Li, X., He, L., Zhang, Y., and Hu, M.: Source apportionment and secondary

413   organic aerosol estimation of PM2.5 in an urban atmosphere in China, Sci. China-Earth Sci., 57, 1352-

414   1362, https://doi.org/10.1007/s11430-013-4686-2, 2014.

415   Jokinen, T., Berndt, T., Makkonen, R., Kerminen, V.-M., Junninen, H., Paasonen, P., Stratmann, F.,

416   Herrmann, H., Guenther, A. B., Worsnop, D. R., Kulmala, M., Ehn, M., and Sipilä, M.: Production of

417   extremely low volatile organic compounds from biogenic emissions: Measured yields and atmospheric

418   implications, Proc. Natl. Acad. Sci. U. S. A., 112, 7123-7128,

419   https://doi.org/doi:10.1073/pnas.1423977112, 2015.

420   Jonsson, A. M., Hallquist, M., and Ljungstrom, E.: Impact of humidity on the ozone initiated oxidation

421   of limonene, Δ^3-carene, and α-pinene, Environ. Sci. Technol., 40, 188-194,

422   https://doi.org/10.1021/es051163w, 2006a.

423   Jonsson, A. M., Hallquist, M., and Ljungstrom, E.: Impact of humidity on the ozone initiated oxidation

424   of limonene, Delta(3)-carene, and alpha-pinene, Environ. Sci. Technol., 40, 188-194,

425   https://doi.org/10.1021/es051163w, 2006b.

426   Jonsson, A. M., Hallquist, M., and Ljungstrom, E.: Influence of OH scavenger on the water effect on

427   secondary organic aerosol formation from ozonolysis of limonene, Δ^3-carene, and α-pinene, Environ. Sci.

428   Technol., 42, 5938-5944, https://doi.org/10.1021/es702508y, 2008.

429   Kanakidou, M., Seinfeld, J. H., Pandis, S. N., Barnes, I., Dentener, F. J., Facchini, M. C., Van Dingenen,

430   R., Ervens, B., Nenes, A., Nielsen, C. J., Swietlicki, E., Putaud, J. P., Balkanski, Y., Fuzzi, S., Horth, J.,

431   Moortgat, G. K., Winterhalter, R., Myhre, C. E. L., Tsigaridis, K., Vignati, E., Stephanou, E. G., and

432   Wilson, J.: Organic aerosol and global climate modelling: a review, Atmos. Chem. Phys., 5, 1053-1123,

433   https://doi.org/10.5194/acp-5-1053-2005, 2005.

434   Khamaganov, V. G. and Hites, R. A.: Rate constants for the gas-phase reactions of ozone with isoprene,

435   α- and β-pinene, and limonene as a function of temperature, J. Phys. Chem. A, 105, 815-822,

436   https://doi.org/10.1021/jp002730z, 2001.

437   Kristensen, K., Cui, T., Zhang, H., Gold, A., Glasius, M., and Surratt, J. D.: Dimers in α-pinene secondary

438   organic aerosol: effect of hydroxyl radical, ozone, relative humidity and aerosol acidity, Atmos. Chem.

439   Phys., 14, 4201-4218, https://doi.org/10.5194/acp-14-4201-2014, 2014.

440   Kumar, M., Busch, D. H., Subramaniam, B., and Thompson, W. H.: Role of tunable acid catalysis in

441   decomposition of α-Hydroxyalkyl hydroperoxides and mechanistic implications for tropospheric

442   chemistry, J. Phys. Chem. A, 118, 9701-9711, https://doi.org/10.1021/jp505100x, 2014.

443   Leungsakul, S., Jaoui, M., and Kamens, R. M.: Kinetic Mechanism for Predicting Secondary Organic

444   Aerosol Formation from the Reaction of d-Limonene with Ozone, Environ. Sci. Technol., 39, 9583-9594,

445   https://doi.org/10.1021/es0492687, 2005.

446   Levy, H., II, Horowitz, L. W., Schwarzkopf, M. D., Ming, Y., Golaz, J.-C., Naik, V., and Ramaswamy,

447   V.: The roles of aerosol direct and indirect effects in past and future climate change, J. Geophys. Res.-

448   Atmos., 118, 4521-4532, https://doi.org/10.1002/jgrd.50192, 2013.

449   Li, J. Y., Zhang, H. W., Ying, Q., Wu, Z. J., Zhang, Y. L., Wang, X. M., Li, X. H., Sun, Y. L., Hu, M.,

450   Zhang, Y. H., and Hu, J. L.: Impacts of water partitioning and polarity of organic compounds on

451   secondary organic aerosol over eastern China, Atmos. Chem. Phys., 20, 7291-7306,

452   https://doi.org/10.5194/acp-20-7291-2020, 2020.

453   Li, K., Liggio, J., Lee, P., Han, C., Liu, Q., and Li, S.-M.: Secondary organic aerosol formation from α-

454   pinene, alkanes, and oil-sands-related precursors in a new oxidation flow reactor, Atmos. Chem. Phys.,

455   19, 9715-9731, https://doi.org/10.5194/acp-19-9715-2019, 2019a.

456   Li, X., Chee, S., Hao, J., Abbatt, J. P. D., Jiang, J., and Smith, J. N.: Relative humidity effect on the

457   formation of highly oxidized molecules and new particles during monoterpene oxidation, Atmos. Chem.

458   Phys., 19, 1555-1570, https://doi.org/10.5194/acp-19-1555-2019, 2019b.

459   Ma, Y., Porter, R. A., Chappell, D., Russell, A. T., and Marston, G.: Mechanisms for the formation of

460   organic acids in the gas-phase ozonolysis of 3-carene, Phys. Chem. Chem. Phys., 11, 4184-4197,

461   https://doi.org/10.1039/b818750a, 2009.

462   Molteni, U., Bianchi, F., Klein, F., El Haddad, I., Frege, C., Rossi, M. J., Dommen, J., and Baltensperger,

463   U.: Formation of highly oxygenated organic molecules from aromatic compounds, Atmos. Chem. Phys.,

464   18, 1909-1921, https://doi.org/10.5194/acp-18-1909-2018, 2018.

465   Mot, M.-D., Gavrilaş, S., Lupitu, A. I., Moisa, C., Chambre, D., Tit, D. M., Bogdan, M. A., Bodescu, A.-

466   M., Copolovici, L., Copolovici, D. M., and Bungau, S. G.: Salvia officinalis L. essential oil:

467   characterization, antioxidant properties, and the effects of aromatherapy in adult patients, Antioxidants,

468   11, 808, https://doi.org/10.3390/antiox11050808, 2022.

469   Ng, N. L., Kroll, J. H., Chan, A. W. H., Chhabra, P. S., Flagan, R. C., and Seinfeld, J. H.: Secondary

470   organic aerosol formation from m-xylene, toluene, and benzene, Atmos. Chem. Phys., 7, 3909-3922,

471   https://doi.org/10.5194/acp-7-3909-2007, 2007.

472   Odum, J. R., Hoffmann, T., Bowman, F., Collins, D., Flagan, R. C., and Seinfeld, J. H.: Gas/particle

473   partitioning and secondary organic aerosol yields, Environ. Sci. Technol., 30, 2580-2585,

474   https://doi.org/10.1021/es950943+, 1996.

475   Palm, B. B., Campuzano-Jost, P., Ortega, A. M., Day, D. A., Kaser, L., Jud, W., Karl, T., Hansel, A.,

476   Hunter, J. F., Cross, E. S., Kroll, J. H., Peng, Z., Brune, W. H., and Jimenez, J. L.: In situ secondary

477   organic aerosol formation from ambient pine forest air using an oxidation flow reactor, Atmos. Chem.

478   Phys., 16, 2943-2970, https://doi.org/10.5194/acp-16-2943-2016, 2016.

479   Pathak, R. K., Salo, K., Emanuelsson, E. U., Cai, C., Lutz, A., Hallquist, A. M., and Hallquist, M.:

480   Influence of ozone and radical chemistry on limonene organic aerosol production and thermal

481   characteristics, Environ. Sci. Technol., 46, 11660-11669, https://doi.org/10.1021/es301750r, 2012.

482   Peng, Z., Lee-Taylor, J., Orlando, J. J., Tyndall, G. S., and Jimenez, J. L.: Organic peroxy radical

483   chemistry in oxidation flow reactors and environmental chambers and their atmospheric relevance,

484   Atmos. Chem. Phys., 19, 813-834, https://doi.org/10.5194/acp-19-813-2019, 2019.

485   Pye, H. O. T., Ward-Caviness, C. K., Murphy, B. N., Appel, K. W., and Seltzer, K. M.: Secondary organic

486   aerosol association with cardiorespiratory disease mortality in the United States, Nat. Commun., 12,

487   https://doi.org/10.1038/s41467-021-27484-1, 2021.

488   Ravichandran, C., Badgujar, P. C., Gundev, P., and Upadhyay, A.: Review of toxicological assessment of

489   d-limonene, a food and cosmetics additive, Food Chem. Toxicol., 120, 668-680,

490   https://doi.org/10.1016/j.fct.2018.07.052, 2018.

491   Sbai, S. E. and Farida, B.: Photochemical aging and secondary organic aerosols generated from limonene

492   in an oxidation flow reactor, Environ. Sci. Pollut. Res., 26, 18411-18420, https://doi.org/10.1007/s11356-

493   019-05012-5, 2019.

494   Seinfeld, J. H., Erdakos, G. B., Asher, W. E., and Pankow, J. F.: Modeling the formation of secondary

495   organic aerosol (SOA). 2. The predicted effects of relative humidity on aerosol formation in the α-Pinene-,

496   β-Pinene-, sabinene-, Δ^3-Carene-, and cyclohexene-ozone systems, Environ. Sci. Technol., 35, 1806-

497   1817, https://doi.org/10.1021/es001765+, 2001.

498   Shaw, J. T., Lidster, R. T., Cryer, D. R., Ramirez, N., Whiting, F. C., Boustead, G. A., Whalley, L. K.,

499   Ingham, T., Rickard, A. R., Dunmore, R. E., Heard, D. E., Lewis, A. C., Carpenter, L. J., Hamilton, J. F.,

500   and Dillon, T. J.: A self-consistent, multivariate method for the determination of gas-phase rate

501   coefficients, applied to reactions of atmospheric VOCs and the hydroxyl radical, Atmos. Chem. Phys.,

502   18, 4039-4054, https://doi.org/10.5194/acp-18-4039-2018, 2018.

503   Sindelarova, K., Granier, C., Bouarar, I., Guenther, A., Tilmes, S., Stavrakou, T., Müller, J. F., Kuhn, U.,

504   Stefani, P., and Knorr, W.: Global data set of biogenic VOC emissions calculated by the MEGAN model

505   over the last 30 years, Atmos. Chem. Phys., 14, 9317-9341, https://doi.org/10.5194/acp-14-9317-2014,

506   2014.

507   Sun, Y., Wang, Z., Fu, P., Jiang, Q., Yang, T., Li, J., and Ge, X.: The impact of relative humidity on

508   aerosol composition and evolution processes during wintertime in Beijing, China, Atmos. Environ., 77,

509   927-934, https://doi.org/10.1016/j.atmosenv.2013.06.019, 2013.

510   Thomsen, D., Elm, J., Rosati, B., Skonager, J. T., Bilde, M., and Glasius, M.: Large discrepancy in the

511   formation of secondary organic aerosols from structurally similar monoterpenes, ACS Earth Space

512   Chem., 5, 632-644, https://doi.org/10.1021/acsearthspacechem.0c00332, 2021.

513   Varutbangkul, V., Brechtel, F. J., Bahreini, R., Ng, N. L., Keywood, M. D., Kroll, J. H., Flagan, R. C.,

514   Seinfeld, J. H., Lee, A., and Goldstein, A. H.: Hygroscopicity of secondary organic aerosols formed by

515   oxidation of cycloalkenes, monoterpenes, sesquiterpenes, and related compounds, Atmos. Chem. Phys.,

516   6, 2367-2388, https://doi.org/10.5194/acp-6-2367-2006, 2006.

517   Wang, L. Y. and Wang, L. M.: The oxidation mechanism of gas-phase ozonolysis of limonene in the

518   atmosphere, Phys. Chem. Chem. Phys., 23, 9294-9303, https://doi.org/10.1039/d0cp05803c, 2021.

519   Watne, A. K., Westerlund, J., Hallquist, A. M., Brune, W. H., and Hallquist, M.: Ozone and OH-induced

520   oxidation of monoterpenes: Changes in the thermal properties of secondary organic aerosol (SOA), J.

521   Aerosol Sci, 114, 31-41, https://doi.org/10.1016/j.jaerosci.2017.08.011, 2017.

522   Xu, L., Tsona, N. T., and Du, L.: Relative humidity changes the role of SO_2 in biogenic secondary organic

523   aerosol formation, J. Phys. Chem. Lett., 12, 7365-7372, https://doi.org/10.1021/acs.jpclett.1c01550,

524   2021.

525   Ye, J., Abbatt, J. P. D., and Chan, A. W. H.: Novel pathway of SO_2 oxidation in the atmosphere: reactions

526   with monoterpene ozonolysis intermediates and secondary organic aerosol, Atmos. Chem. Phys., 18,

527   5549-5565, https://doi.org/10.5194/acp-18-5549-2018, 2018.

528   Yu, K. P., Lin, C. C., Yang, S. C., and Zhao, P.: Enhancement effect of relative humidity on the formation

529   and regional respiratory deposition of secondary organic aerosol, J. Hazard. Mater., 191, 94-102,

530   https://doi.org/10.1016/j.jhazmat.2011.04.042, 2011.

531   Zhang, H., Wang, S., Hao, J., Wang, X., Wang, S., Chai, F., and Li, M.: Air pollution and control action

532   in Beijing, J. Clean Prod., 112, 1519-1527, https://doi.org/10.1016/j.jclepro.2015.04.092, 2016.

533   Zhao, R. R., Zhang, Q. X., Xu, X. Z., Zhao, W. X., Yu, H., Wang, W. J., Zhang, Y. M., and Zhang, W. J.:

534   Effect of experimental conditions on secondary organic aerosol formation in an oxidation flow reactor,

535   Atmos. Pollut. Res., 12, 392-400, https://doi.org/10.1016/j.apr.2021.01.011, 2021.

536   Ziemann, P. J. and Atkinson, R.: Kinetics, products, and mechanisms of secondary organic aerosol

537   formation, Chem. Soc. Rev., 41, 6582-6605, https://doi.org/10.1039/c2cs35122f, 2012.

538